Available online at www.sciencedirect.com
SCIENCE DIRECT®
Journal of Molecular Catalysis A: Chemical 230 (2005) 151–157
JOURNAL OF MOLECULAR CATALYSIS A: CHEMICAL
www.elsevier.com/locate/molcata

ortho-Selective ethylation of phenol with ethanol catalyzed by bimetallic mesoporous catalyst, CoAl-MCM-41

Ajayan Vinu[a,*], Mani Karthik[b], Masahiko Miyahara[c], Velayudam Murugesan[b], Katsuhiko Ariga[c]

[a] *International Center for Young Scientists (ICYS), National Institute for Materials Science (NIMS), 1-1 Namiki, Tsukuba 305-0044, Japan*
[b] *Department of Chemistry, Anna University, Guindy, Chennai 600 025, India*
[c] *Supermolecules Group, Advanced Materials Laboratory (AML), National Institute for Materials Science (NIMS), 1-1 Namiki, Tsukuba 305-0044, Japan*

Received 27 November 2004; received in revised form 18 December 2004; accepted 19 December 2004
Available online 26 January 2005

Abstract

CoAl-MCM-41 (*X*) catalysts with $X = n_{Si}/(n_{Co} + n_{Al})$ various ratios were synthesized and ethylation of phenol with ethanol was studied in vapor-phase at temperatures between 250 and 450 °C. The products obtained were *O*-alkylated product (ethyl phenyl ether), *C*-alkylated products (2-ethylphenol and 4-ethylphenol), and *C*-/*O*-alkylated products (ethyl ethylphenyl ether). The phenol conversion increased significantly with reaction temperature over all the catalysts. The activity of the catalysts followed the order CoAl-MCM-41 (20) > CoAl-MCM-41 (50) > CoAl-MCM-41 (80). Selectivity between the *C*-alkylation and the *O*-alkylation depended on the factors such as acidity of the catalyst and the reaction temperature. CoAl-MCM-41 (20) catalyst displayed a phenol conversion of 40% and a selectivity of more than 80% for 2-ethylphenol under the optimized reaction condition. The ethanol to phenol ratios and the reactant flow rate are also influential for both activity and selectivity of CoAl-MCM-41 catalysts.

Keywords: Ethylation; Phenol; *C*-alkylation; *ortho*-Selectivity; CoAl-MCM-41

1. Introduction

Alkyl phenols are industrially important chemicals that are used directly or as intermediates in the syntheses of drugs pharmaceuticals, and photo-active dyes [1,2]. Ethylation of phenol is reaction indispensable for production of phenolic resins. For instance, 2-ethylphenol is used as a starting material for production of indene-coumarone resins and some pharmaceuticals. Generally, phenol alkylation is carried out over the conventional acid catalysts such as $AlCl_3$, phosphoric acid, sulfuric acid and cation exchange resins [3]. The major drawbacks of homogeneous catalysts employed in this reaction are their hazardous nature and the required separation of the catalyst from the reaction mixture after the reaction. On the other hand, cationic exchange resins cannot be used because of their lower stability at higher temperature as well as their low activity and selectivity. Zeolite catalysts and sulfated zirconia were also applied for the phenol alkylation, but sometimes undergo deactivation significantly with time-on-stream due to the formation of coke from phenol or alkylating agent [4,5].

As modern approaches, mesoporous media is used as a unique environment for immobilization of functional units and for materials conversion [6–19]. Among numerous examples, use of the mesoporous silica as catalytic medium seems to be one of the most fruitful directions in practical usages [20–26]. In fact, mesoporous materials have also been used for matrices of catalysts of the above-mentioned phenol alkylation [27–32]. The selectivity of various products in the mesoporous catalyst depends on several factors: pore geometry, nature and the coordination of metal species, reaction parameters, and alkylating reagents. Very recently, Murugesan

* Corresponding author. Tel.: +81 29 851 3354x8679; fax: +81 29 860 4706.
E-mail address: vinu.ajayan@nims.go.jp (A. Vinu).

1381-1169/$ – see front matter © 2004 Elsevier B.V. All rights reserved.
doi:10.1016/j.molcata.2004.12.018

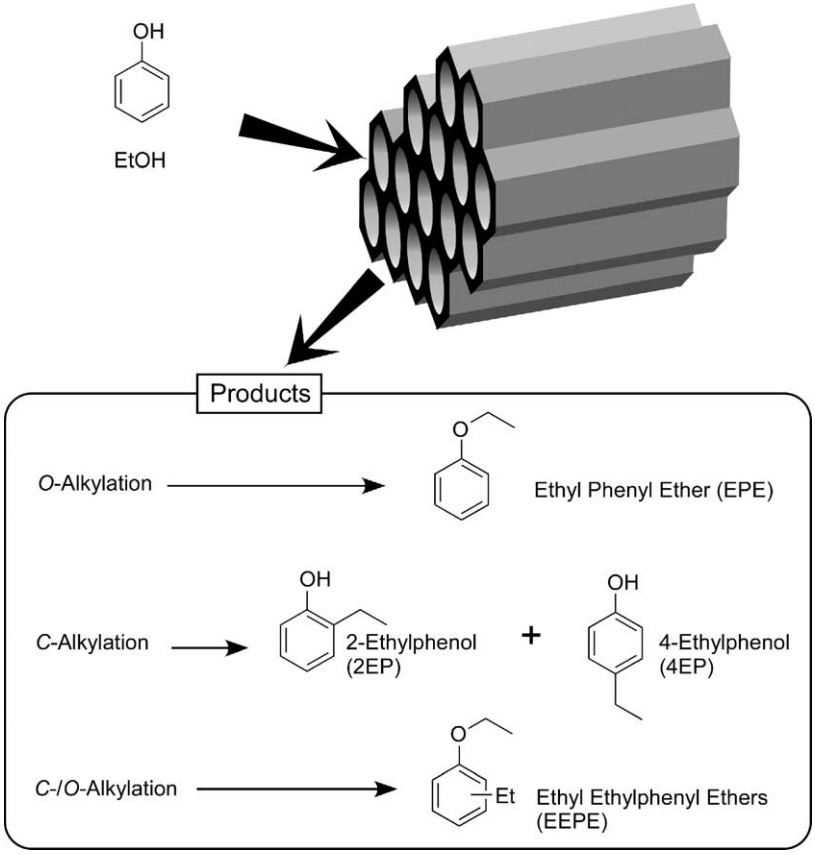

Fig. 1. Products of phenol ethylation investigated in this research.

and coworkers have reported the acidity control of bimetallic mesoporous catalyst, CoAl-MCM-41, and demonstrated activity of *tert*-butylation of phenol using isobutanol [30]. Incorporation of cobalt into framework of Al-MCM-41 led to generate moderate acidic sites and modified reaction selectivity.

In the present work, the behavior of the mesoporous catalyst, CoAl-MCM-41 in the vapor-phase ethylation of phenol (Fig. 1) has been investigated. Samples with different $n_{Si}/(n_{Co} + n_{Al})$ ratio were tested. Their acidity was assessed by FTIR technique using pyridine as probe molecule. CoAl-MCM41 (20) catalyst showed a higher selectivity for *ortho*-substituted phenol, 2-ethyl phenol than *para*-substituted phenol, 4-ethylphenol. The effect of reactant feed ratio, flow rate and time-on-stream on the conversion of phenol and the selectivity of various products over CoAl-MCM-41 was also investigated.

2. Experimental

2.1. Syntheses and characterization of CoAl-MCM-41

CoAl-MCM-41 samples with various $n_{Si}/(n_{Co} + n_{Al})$ ratios (the n_{Co}/n_{Al} was fixed to 1) were synthesized from gels with the following gel composition – $10SiO_2$:$5.4C_{14}$TMABr:$0.003–0.0125Al_2O_3$:$0.006–0.025CoO$:$4.25Na_2O$:$1.3H_2SO_4$:$480H_2O$, according to the reported method. The obtained materials were denoted as CoAl-MCM-41 (*X*), where *X* represents $n_{Si}/(n_{Co} + n_{Al})$. The powder X-ray diffraction patterns of the CoAl-MCM-41 materials were collected on a Siemens D5005 diffractometer using Cu Kα ($\lambda = 0.154$ nm) radiation. The diffractograms were recorded in the 2θ range of 0.8–10° with a two step size of 0.01° and a step time of 10 s. Nitrogen adsorption and desorption isotherms were collected at −196 °C on a Quantachrome Autosorb 1 sorption analyzer. All samples were outgassed for 3 h at 250 °C under vacuum ($p < 10^{-5}$ hPa) in the degas port of the adsorption analyzer. The specific surface area was calculated using the BET model. DRIFT spectra of the samples were recorded on a Nicolet (Avatar 360) FT-IR spectrophotometer equipped with a high temperature vacuum chamber. Approximately 30 mg of the sample was taken in the sample holder and dehydrated at 400 °C for 6 h under vacuum (10^{-5} mbar). The sample was then cooled to room temperature and the spectra were recorded. Then pyridine was adsorbed at room temperature. The physisorbed pyridine was removed by heating the sample at 150 °C under vacuum (10^{-5} mbar) for 30 min, after the sample was cooled to room temperature, the spectrum was recorded. The number of Brønsted and Lewis acid sites was calculated by measuring the integrated absorbance of bands

representing pyridinium ion formation and coordinatively bonded pyridine [33]. The method developed for porous aluminosilicates by Emeis was adopted for the determination of the acidity of the catalysts [34].

2.2. Catalytic study

The reactor system was a fixed-bed, vertical, down ward-flow type made up of a quartz tube of 40 cm length and 2 cm in internal diameter. The reactor was heated to the requisite temperature with the help of a tubular furnace controlled by a digital temperature controller cum indicator. The temperature was measured by a chromal–alumel thermocouple placed inside the furnace. The catalysts were pressed without binder, crushed and sieved to obtain particles with a size of 250–350 μm. About 0.5 g of the catalyst was placed in the reactor and supported on either side with a thin layer of quartz wool and ceramic beads. The reactants were fed into the reactor using a syringe infusion pump that could be operated at different flow rates. The reaction was carried out at atmospheric pressure. The liquid products collected in the first 15 min were discarded and the analysis was made only with the products collected after this time. After each catalytic run, the catalyst was regenerated by passing moisture and carbon dioxide free air through the reactor for 6 h at 500 °C. The liquid products were analyzed using a Shimadzu gas chromatograph GC-17A using DB-5 capillary column (30 m) equipped with flame ionization detector (FID) and nitrogen as a carrier gas. The identification of products was also made using GC-MS (Perkin Elmer Auto System XL Gas Chromatograph (Perkin Elmer elite series PE-5 capillary column, 30 m × 0.25 mm × 1 μm) equipped with Turbo Mass Spectrometer (EI, 70 eV) with helium as carrier gas at a flow rate of 1 mL min^{-1}).

3. Results and discussion

3.1. Catalyst characterization

The well defined XRD patterns of calcined CoAl-MCM-41 materials with clear four XRD reflections (1 0 0), (1 1 0), (2 0 0) and (2 1 0) as indexed to a hexagonal lattice were observed (see Appendix B). The n_{Si}/n_{Al} and n_{Si}/n_{Co} molar ratios of all the synthesized materials were in close agreement with the input gel compositions. For the catalysis study, three samples, CoAl-MCM-41 (20), CoAl-MCM-41 (50), and CoAl-MCM-41 (80) were used, where indexes 20, 50, and 80 represent $n_{Si}/(n_{Co} + n_{Al})$ ratios. The nitrogen adsorption isotherms of the CoAl-MCM-41 materials exhibit a type IV isotherm of the IUPAC classification featuring a narrow step due to capillary condensation of N_2 in the primary mesopores. The incorporation of Co and Al into the walls of MCM-41 has a significant effect on the specific surface area, and specific pore volume of the materials. With increasing metal content, the pore volume is reduced from 0.85 to 0.66 $cm^3\ g^{-1}$ and the specific surface area declines from 1270 to 1015 $m^2\ g^{-1}$. The pore diameter of CoAl-MCM-41 samples is larger than the pure silica MCM-41. The pore diameter of CoAl-MCM-41 (20) is smaller than CoAl-MCM-41 (50) and CoAl-MCM-41 (80). This could be due to the formation of more metal oxide clusters in the mesopores of CoAl-MCM-41 (20). Structural parameters of CoAl-MCM-41 are summarized in Table 1.

The acid sites of these catalysts were obtained by in situ DRIFT upon pyridine adsorption. The acidity of the catalysts was calculated using extinction coefficients of the bands of Brønsted and Lewis acid sites adsorbed pyridine. The obtained values are also summarized in Table 1. With increasing cobalt content, the number of both Brønsted and Lewis surface acid sites increases, i.e., the acidity of the catalysts decreases in the order CoAl-MCM-41 (20) > CoAl-MCM-41 (50) > CoAl-MCM-41 (80). Therefore, it is concluded that the isomorphic substitution of Co^{2+} into the framework of mesoporous Al-MCM-41 creates more acid sites (Brønsted and Lewis).

3.2. General tendency of catalysis: effect of temperature

Effects of temperature on phenol conversion for all the catalysts at a temperature range between 250 and 450 °C are summarized in Fig. 2. The phenol conversion increases from 250 to 400 °C, but above 400 °C it decreases. The less conversion at low temperature is mainly attributed to the molecular association that reduces adsorption and dissociation on the active sites. The decrease in conversion above 400 °C is attributed to predominant dealkylation over alkylation at higher temperature and blocking of active sites by thin films of polyethylene oligomers [5]. Especially, it is commonly known for the alkylation of phenol and its derivatives that coke formation seriously disturbs the reaction [32]. Among three catalysts, CoAl-MCM-41 (20) showed apparently high catalytic performance. As the reaction requires formation of ethyl cation for electrophilic attack on either the chemisorbed phenol or the free phenol [35], the density of acid sites is im-

Table 1
Structural features of CoAl-MCM-41 (*X*) [30]

X	Pore structure			Acid site nature	
	Surface area ($m^2\ g^{-1}$)	Pore diameter (nm)	Pore volume ($cm^3\ g^{-1}$)	Brønsted, *B* (mmol g^{-1})	Lewis, *L* (mmol g^{-1})
20	1015	2.44	0.66	0.190	0.284
50	1099	2.49	0.74	0.117	0.107
80	1147	2.49	0.77	0.057	0.026

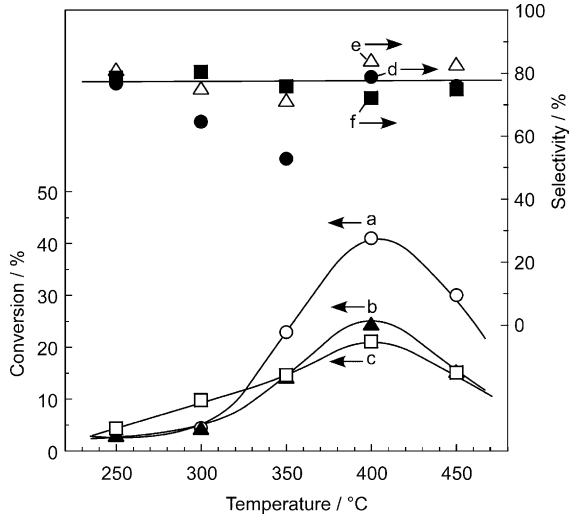

Fig. 2. Effects of temperature on the phenol ethylation, conversion of phenol and *ortho*-selectivity in *C*-alkylated products ([2EP]/([2EP] + [4EP]) × 100): (a) conversion of phenol with CoAl-MCM-41 (20); (b) conversion of phenol with CoAl-MCM-41 (50); (c) conversion of phenol with CoAl-MCM-41 (80); (d) *ortho*-selectivity with CoAl-MCM-41 (20); (e) *ortho*-selectivity with CoAl-MCM-41 (50); (f) *ortho*-selectivity with CoAl-MCM-41 (80). Reaction condition: [EtOH]/[PhOH], 3/1; feed rate, 2 mL h^{-1}; catalyst weight, 0.5 g.

portant as active site for this reaction. CoAl-MCM-41 (20) has the highest density of acid sites, as shown in Table 1, and showed the highest activity on the ethylation of phenol.

Compositions of *O*-alkylated product (ethyl phenyl ether, EPE), *C*-alkylated products (2-ethylphenol, 2EP and 4-ethylphenol, 4EP), and *C*-/*O*-alkylated products (ethyl ethylphenyl ether, EEPE) are summarized in Fig. 2. Basically, the *C*-alkylated products occupies majority under conditions investigated. At low temperature, the *O*-alkylated product can be detected, but vanishes as the reaction temperature increased. In contrast, two-point reaction, which produces the *C*-/*O*-alkylated products, cannot be ignored at higher temperature. CoAl-MCM-41 (20) is the best catalyst for the *C*-alkylation. For example, more than 90% of the products are the *C*-alkylated ones with CoAl-MCM-41 (20) at 300 °C.

The alkylation of phenol is generally reported to be sensitive to the acid-base natures of the catalytic sites. It has been reported that the *C*-alkylation of phenol preferentially proceeds at weak acidic or strong basic sites [36], while the *O*-alkylation is favored at strong acid site [37]. Some research groups claimed that the weak acid sites are important for the *C*-alkylation [38,39] and other researchers reported that the *C*-alkylation is promoted by higher acidity. It is known that incorporation of Co^{2+} into framework of MCM-41 leads to moderate acidity [30]. Therefore, CoAl-MCM-41 (20) should have moderate acidic sites in high density, resulting in high probability of the *C*-alkylation. The obtained tendency basically agrees with *tert*-butylation of phenol in the previous report [30].

As summarized in Table 1, both Brønsted and Lewis acidic sites are increased at high content of Co/Al. Among them, the Lewis acid site could induce the *O*-alkylation through nucleophilic attack of adsorbed phenolate to ethyl cation [30]. However, the increased production of the *O*-alkylated compound was not observed in CoAl-MCM-41 (20) catalyst, although it has the highest content of the Lewis acid sites. The obtained result may suggest that the Brønsted acid site plays more important role in the phenol ethylation with this catalyst.

Next, *para*- and *ortho*-selectivity was examined within the *C*-alkylated products as summarized in Fig. 2. Although some of the data have some scattering, apparent preferential *ortho*-selectivity, compared to statistic ratio, was observed regardless of the reaction temperature and Co content in the catalyst. This *ortho*-selectivity is discussed in the later section.

3.3. Effect of WHSV, feed ratio, and time-on-stream

The influence of weight hourly space velocity (WHSV) on phenol conversion and product selectivity over CoAl-MCM-41 (20) was also studied at 400 °C. Conversion and product selectivities at different WHSV ranging from 2 to 6 h^{-1} (based on phenol) are shown in Fig. 3. When the WHSV is increased from 2 to 6 h^{-1}, the conversion of phenol increases first and then decreases significantly at a higher WHSV 5.65 h^{-1} (Fig. 3A). Low conversion of phenol at higher WHSV could be due to high diffusion of the reactant molecules whereas less conversion at low WHSV could be attributed to the dealkylation of ethyl phenol and coke formation due to the longer contact times. In these conditions, *C*-alkylation is dominant and independent from WHSV values (Fig. 3B). It can be also seen from Fig. 3C that the selectivity for 2-EP increases as the WHSV increases from 2.6 to 3.8 h^{-1}, and decreases at a higher WHSV of 5.65 h^{-1}.

The effect of feed ratio, [EtOH]/[PhOH], was similarly investigated using CoAl-MCM-41 (20) as a catalyst at 400 °C. The conversion of phenol increased when sufficient amount of EtOH (ethanol), compared to PhOH (phenol), as expected (Fig. 4A). However, too much presence of EtOH conversely decreased the conversion, which may be caused from competition between EtOH and PhOH in accessibility to catalytic sites. Increase of EtOH content also induced additional *O*-alkylation to the *C*-alkylated products (2EPE and 4EPE) resulting in EEPE (Fig. 4B). However, increment of EEPE was not observed although EtOH content was increased by fivefold. This tendency implies that the *C*-alkylation is dominant under the used catalyst system. Similarly to the abovementioned case (Fig. 2), the *ortho*-selectivity (2EP content in the *C*-alkylated products) is ca. 80% as shown in Fig. 4C.

The effect of time-on-stream was also examined using CoAl-MCM-41 (20) as a catalyst at 400 °C with a fixed feed ratio ([EtOH]/[PhOH] = 3). There is only a slight decrease in the conversion of phenol with time-on-stream indicating the stability of the catalyst towards deactivation by coke formation though the reaction is carried out at a high reaction temperature, 400 °C (Fig. 5A). As seen in Fig. 5B and C,

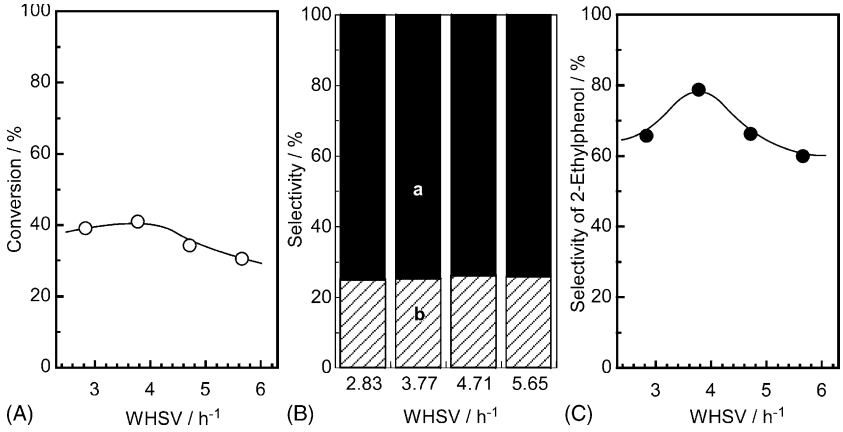

Fig. 3. Effect of WHSV (feed rate): (A) phenol conversion; (B) composition of product [(a) *C*-alkylated products 2EP and 4EP; (b) *C*-/*O*-alkylated products EEPE]; (C) *ortho*-selectivity in *C*-alkylated products ([2EP]/([2EP] + [4EP]) × 100). Reaction condition: [EtOH]/[PhOH], 3/1; temperature, 400 °C; CoAl-MCM-41 (20), 0.5 g. WHSV values of 2.83, 3.77, 4.71, and 5.65 h^{-1} correspond to feed rate of 1.5, 2.0, 2.5, and 3.0 mL h^{-1}, respectively.

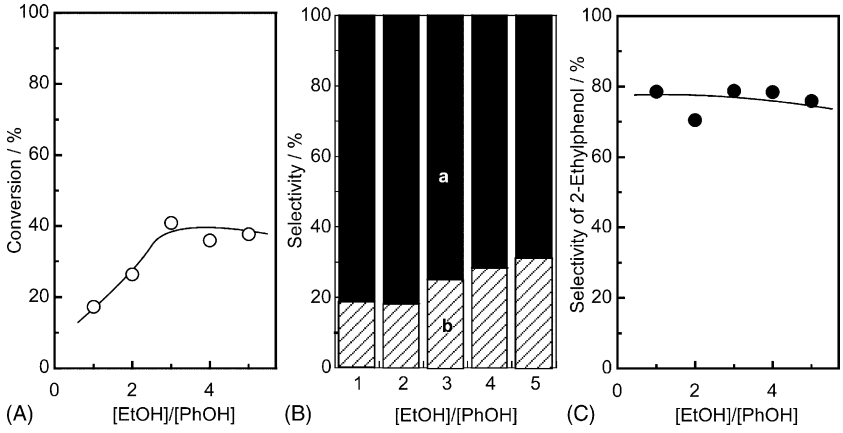

Fig. 4. Effect of feed ratio, [EtOH]/[PhOH]: (A) phenol conversion; (B) composition of product [(a) *C*-alkylated products 2EP and 4EP; (b) *C*-/*O*-alkylated products EEPE]; (C) *ortho*-selectivity in *C*-alkylated products ([2EP]/([2EP] + [4EP]) × 100). Reaction condition: feed rate, 2 mL h^{-1}; temperature, 400 °C; CoAl-MCM-41 (20), 0.5 g.

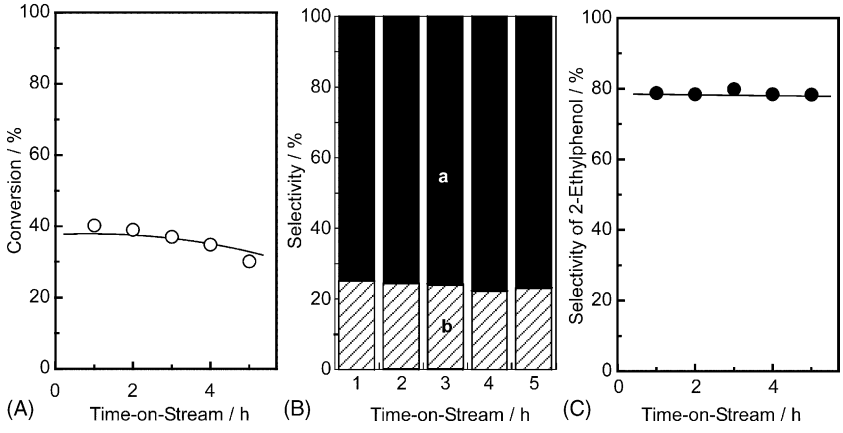

Fig. 5. Effect of time-on-stream: (A) phenol conversion; (B) composition of product [(a) *C*-alkylated products 2EP and 4EP; (b) *C*-/*O*-alkylated products EEPE]; (C) *para*-selectivity in *C*-alkylated products ([2EP]/([2EP] + [4EP]) × 100). Reaction condition: [EtOH]/[PhOH], 3/1; temperature, 400 °C; CoAl-MCM-41 (20), 0.5 g.

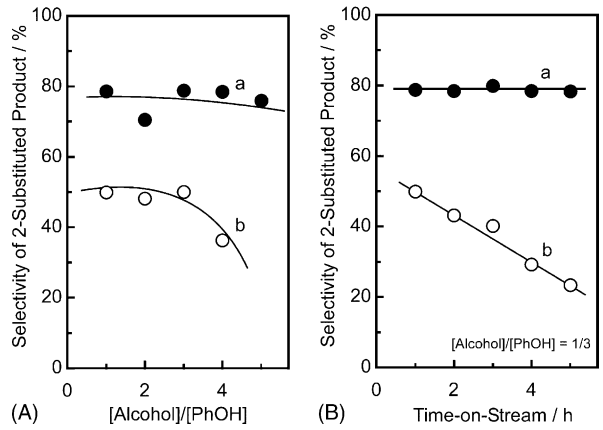

Fig. 6. Comparison of *ortho*-selectivity (percentage of two-substituted compound in *C*-alkylated products) between phenol ethylation (a) and phenol *tert*-butylation (b): (A) effect of feed ratio; (B) effect of time-on-stream. Reaction condition: temperature, 400 °C; CoAl-MCM-41 (20), 0.5 g.

predominance of the *C*-alkylation and the *ortho*-selectivity in phenol ethylation were observed regardless of the time-on-stream.

3.4. Regio-selectivity (ortho-/meta-/para-selectivity)

In most of the cases investigated here, *ortho*-selective nature is recognized in the *C*-monoethylated phenols. The *ortho*-selectivity is ca. 80% in the most of the cases and apparently larger than statistic selectivity (66.7%). The preferential selectivity of the *ortho*-product compared to thermodynamically stable *meta*-product could be due to the fact that the hydroxyl group on the phenol provides *ortho*/*para* directing tendency. Though the OH group on the phenol is *ortho*/*para* directing, the selectivity towards the *para*-product is much lower than the *ortho*-product in the most cases investigated. This could be due to relative orientation of phenol and ethyl cation. Phenol approaches ethyl cation on the catalyst surface through its OH group pointing towards the channel surface, which would help the *ortho*-position of phenol molecule more susceptible to the electrophilic reaction with ethyl cation [32].

It is also interesting to compare the results of phenol ethylation with those observed for the phenol *tert*-butylation. The *ortho*-selectivity observed in this research is apparently opposite to the case of *tert*-butylation of phenol, using the same catalyst, where *para*-substitution is dominant [30]. In order to clearly compare two systems, *ortho*-selectivity in the *C*-alkylated products is summarized in Fig. 6 for both ethylation and *tert*-butylation [30] of phenol using the same CoAl-MCM-41 catalyst. The ethylation of phenol keeps *ortho*-selectivity regardless of feed ratios and time-on-stream, while *para*-substitution is dominant, depending on reaction condition, in the phenol butylation. Phenol and/or phenolate could adsorb perpendicularly to the acid site and carbocation generated in neighbor site attack the adsorbed phenol [36,40,41]. Small ethyl cation preferably attacks *ortho*-position of the phenol due to proximity effect. In contrast, bulky *tert*-butyl cation cannot easily attack *ortho*-position because of large steric hindrance, resulting in *para*-preferential substitution [35]. In addition, more stable and long-lived *tert*-butyl cation has higher probability to reach the *para*-position of phenol at far site.

4. Conclusion

In this research, we applied bimetallic mesoporous catalysts, CoAl-MCM-41 to the ethylation of phenol. Selectivity between the *C*-alkylation and the *O*-alkylation depended on the factors such as metal content and temperature. The *C*-alkylation is generally dominant, and more than 90% of the products can be assigned the *C*-alkylated phenols under the optimized reaction condition. Among the *C*-alkylated products, *ortho*-substituted compound occupies majority regardless of the reaction conditions. This tendency is opposite to *para*-selective *tert*-butylation of phenol using the same catalyst, which could be explained through steric factors at the surface catalytic sites. Accumulation of experimental results and knowledge would lead to general guide direction for designer mesoporous catalysts having well-tuned reaction selectivity.

Acknowledgements

A. Vinu is grateful to Prof. Y. Bando and Special Coordination Funds for Promoting Science and Technology from the Ministry of Education, Culture, Sports, Science and Technology of the Japanese Government for the award of ICYS Research Fellowship, Japan.

Appendix A. Supplementary data

Supplementary data associated with this article can be found, in the online version, at 10.1016/j.molcata.2004.12.021.

References

[1] R. Dowbenko, in: J.I. Kroschwitz, Mary Howe-Grant (Eds.), Kirk–Othmer Encyclopedia of Chemical Technology, vol. 2, 4th ed., Wiley, New York, p. 106.
[2] H. Fiege, in: B. Elvers, S. Hawkins, G. Schultz (Eds.), Ullmann's Encyclopedia of Industrial Chemistry, vol. A19, 5th ed., VCH Verlag, 1989, p. 313.
[3] V.A. Koshchii, Y.B. Kozlikovskii, A.A. Matyusha, Zh. Org. Khim. 24 (1989) 1508.
[4] R.A. Rajadhyaksha, D.D. Chaudhari, Ind. Eng. Chem. Res. 26 (1987) 1276.
[5] K. Zhang, C. Huang, H. Zhang, S. Xiang, S. Liu, D. Xu, H. Li, Appl. Catal. A: Gen. 166 (1998) 89.
[6] T. Yanagisawa, T. Shimizu, K. Kuroda, C. Kato, Bull. Chem. Soc. Jpn. 63 (1990) 988.

[7] C.T. Kresge, M.E. Leonowicz, W.J. Roth, J.C. Vartuli, J.S. Beck, Nature 359 (1992) 710.
[8] D. Zhao, P. Yang, Q. Huo, B.F. Chmelka, G.D. Stucky, Curr. Opin. Solid State Mater. Sci. 3 (1998) 111.
[9] A. Sayari, S. Hamoudi, Chem. Mater. 13 (2001) 3151.
[10] M.E. Davis, Nature 417 (2002) 813.
[11] A. Okabe, T. Fukushima, K. Ariga, T. Aida, Angew. Chem. Int. Ed. 41 (2002) 3414.
[12] A. Vinu, C. Streb, V. Murugesan, M. Hartmann, J. Phys. Chem. B 107 (2003) 8297.
[13] A. Vinu, V. Murugesan, O. Tangermann, M. Hartmann, Chem. Mater. 16 (2004) 3056.
[14] A. Vinu, V. Murugesan, M. Hartmann, J. Phys. Chem. B 108 (2004) 7323.
[15] M. Miyahara, A. Vinu, T. Nakanishi, K. Ariga, Kobunshi Ronbunshu 61 (2004) 623.
[16] Q. Zhang, K. Ariga, A. Okabe, T. Aida, J. Am. Chem. Soc. 126 (2004) 988.
[17] K. Ariga, Chem. Rec. 3 (2004) 297.
[18] K. Ariga, J. Nanosci. Nanotechnol. 4 (2004) 23.
[19] A. Okabe, T. Fukushima, K. Ariga, M. Niki, T. Aida, J. Am. Chem. Soc. 126 (2004) 9013.
[20] A. Sayari, Chem. Mater. 8 (1996) 1840.
[21] A. Corma, Chem. Rev. 97 (1997) 2373.
[22] J.Y. Ying, C.P. Mehnert, M.S. Wong, Angew. Chem. Int. Ed. 38 (1999) 56.
[23] M. Hartmann, A. Vinu, S.P. Elangovan, V. Murugesan, W. Böhlmann, Chem. Commun. (2002) 1238.
[24] T. Joseph, S.S. Deshpande, S.B. Halligudi, A. Vinu, S. Ernst, M. Hartmann, J. Mol. Catal. A: Chem. 206 (2003) 13.
[25] M. Karthik, A. Vinu, A.K. Tripathi, N.M. Gupta, M. Palanichamy, V. Murugesan, Microporous Mesoporous Mater. 70 (2004) 15.
[26] A. Vinu, K. Ariga, S. Saravanamurugan, M. Hartmann, V. Murugesan, Microporous Mesoporous Mater. 76 (2004) 91.
[27] K.G. Bhattacharyya, A.K. Talukdar, P. Das, S. Sivasanker, J. Mol. Catal. A: Chem. 197 (2003) 255.
[28] A. Vinu, T. Krithiga, V. Murugesan, M. Hartmann, Adv. Mater. 16 (2004) 1817.
[29] A. Vinu, K.U. Nandhini, V. Murugesan, W. Böhlmann, V. Umamaheswari, A. Pöppl, M. Hartmann, Appl. Catal. A: Gen. 265 (2004) 1.
[30] M. Karthik, A.K. Tripathi, N.M. Gupta, A. Vinu, M. Hartmann, M. Palanichamy, V. Murugesan, Appl. Catal. A: Gen. 268 (2004) 139.
[31] S. Udayakumar, A. Pandurangan, P.K. Sinha, Appl. Catal. A: Gen. 272 (2004) 267.
[32] K. Shanmugapriya, R. Anuradha, M. Palanichamy, B. Arabindoo, V. Murugesan, J. Mol. Catal. A: Chem. 221 (2004) 145.
[33] E.P. Parry, J. Catal. 2 (1963) 371.
[34] C.A. Emesis, J. Catal. 141 (1993) 347.
[35] T. Mathew, S. Shylwsh, B.M. Devassy, M. Vijayaraj, C.V.V. Satyanarayana, B.S. Rao, C.S. Gopinath, Appl. Catal. A: Gen. 273 (2004) 35.
[36] V. Durgakunari, G. Sreekanth, S. Narayanan, Res. Chem. Intermed. 14 (1990) 223.
[37] V.V. Rao, K.V.R. Chary, V. Durgakumari, S. Narayanan, Appl. Catal. 61 (1990) 89.
[38] R. Tleimat-Manzalji, D. Bianchi, G.M. Pajonk, Appl. Catal. A: Gen. 101 (1993) 339.
[39] M. Marczewski, J.-P. Bodibo, G. Perot, M. Guisnet, J. Mol. Catal. 50 (1989) 211.
[40] T. Kotanigawa, Bull. Chem. Soc. Jpn. 47 (1974) 950.
[41] T. Mathew, M. Vijayaraj, S. Pai, B.B. Tope, S.G. Hegde, B.S. Rao, C.S. Gopinath, J. Catal. 227 (2004) 175.